International Journal of Engineering Research & Technology (IJERT)
ISSN: 2278-0181
Vol. 4 Issue 09, September-2015

Optimum Groove Location for Two Groove Hydrodynamic Fluid Film Bearing

Ashutosh Kumar
Indian Institute of Technology,
Guwahati 781039, India

Abstract **- This paper shows the various arrangement for location of groove for two groove hydrodynamic journal bearing for optimum performance. In the present work the effect of different location of oil groove on the performance of hydrodynamic journal bearing has been observed. The basic Reynolds equation is nondimensionalized by using proper substitutions and then it is solved numerically by using finite difference method satisfying the Reynolds boundary condition. Determination of optimum location of groove is based on the maximization of nondimensionalized load carrying capacity and flow coefficient and minimization of friction variable. Initially both the groove has been placed at diametrically opposite directions but in this work the optimum location arrived, are not the diametrically opposite.**

INTRODUCTION:

Journal bearing are having excellent damping characteristics and low wear. Because of this property it is being extensively used in turbo machinery system. When the shaft is rotated at very high speed and also for longer period of time then there will be heat generation. To avoid this continuous supply of lubricating oil is necessary. To provide continuous supply of oil, groove is provided in the bearing but the location of the groove should be properly managed such that we get optimum performance. In the line Raimondi and Boyd [1] solved the finite journal bearing fundamental equations numerically and they presented the results in the form of charts and tables that permit the determination of friction, film thickness, flow, temperature rise, load carrying capacity and other basic parameters for the design of a full finite journal bearing. Vijayraghavan and Keith [2] analyzed the effects of groove type, groove number and groove location on the performance of journal bearing. They considered both axial and circumferential grooves in their analysis. Grooves were arranged symmetrically about axial center of bearing and only one half of bearing was analyzed. Jang *et. al.* [3] investigated the performance of grooved journal bearings. FEM was used to solve the Reynolds equation in order to calculate the pressure distribution in a fluid film. Hirani and Rao [4] studied the location of Groove and the configuration of groove for optimum performance of cylindrical journal bearing. They used Newton-Raphson iterative procedure to predict the journal eccentricity for the given load, speed and bearing configuration. They also considered the effects of cavitation on the bearing performance. They concluded that the optimum location for a 150 circumferential groove is in the divergent region. They concluded that the optimum location of groove depends on the applied speed and load condition. Tsai *et. al.* [5] proposed an enhanced Artificial Bee Colony optimization algorithm, which is called the Interactive Artificial Bee Colony optimization for numerical optimization problem. Murugan and Mohan [6] presented a paper in which they presented a new approach for solving the Combined Heat and Economic Dispatch (CHPED) problem using an artificial bee colony algorithm (ABC). They concluded that ABC has effectively provided the best solution satisfying both equality and inequality constraints.

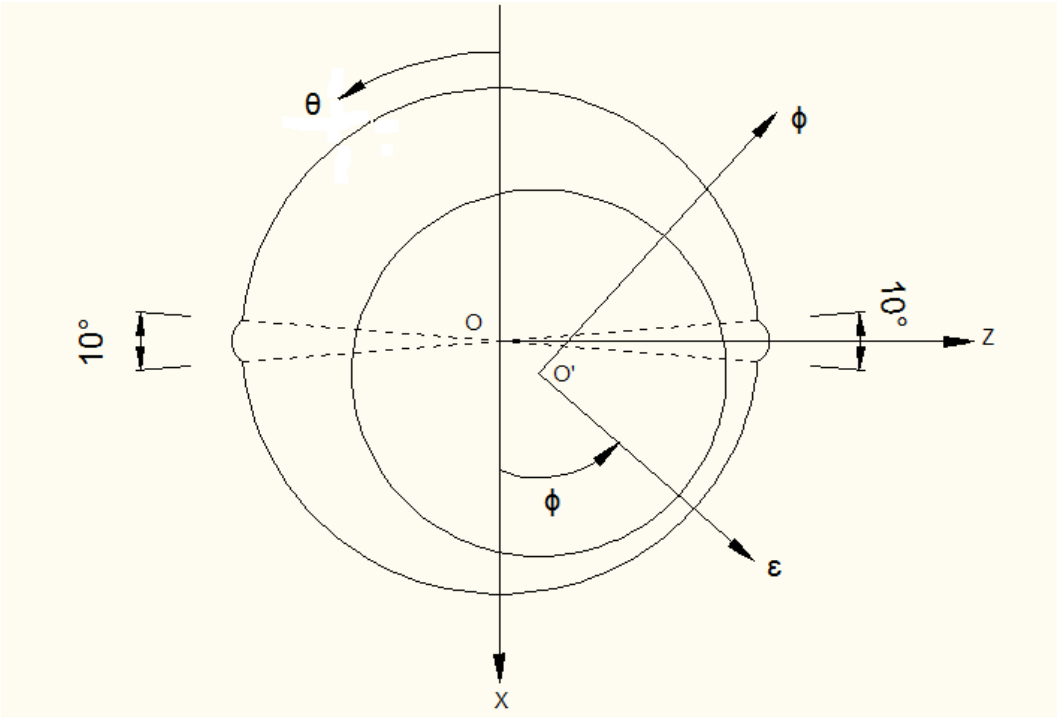

Fig 1: Grooves at diametrically opposite location.

From the literature survey it has been found that groove size of 10^0 has the better performance. In the present work, initially the groove of size 10^0 is placed at diametrically opposite position from 85^0 to 95^0 and from 265^0 to 275^0 respectively. The result is analyzed and further the location of groove is optimized using optimization technique for improved performance characteristics.

Theory:

The governing differential equation for a finite bearing using incompressible lubricant of constant viscosity is given by

$$\frac{\partial}{\partial x}\left(h^3\frac{\partial p}{\partial x}\right)+\frac{\partial}{\partial z}\left(h^3\frac{\partial p}{\partial z}\right)=6\eta U\frac{\partial h}{\partial x} \tag{1}$$

Using substitution as

$$\theta=\frac{x}{R};\qquad \bar{z}=\frac{z}{L/2};\quad \bar{h}=\frac{h}{c};\ \ \bar{p}=\frac{pc^2}{6\eta UR}$$

The following non-dimensional equation has been resulted on substitution of the above,

$$\frac{\partial}{\partial\theta}\left\{\bar{h}^3\frac{\partial\bar{p}}{\partial\theta}\right\}+\left(\frac{D}{L}\right)^2\bar{h}^3\frac{\partial^2\bar{p}}{\partial\bar{z}^2}=\frac{d\bar{h}}{d\theta} \tag{2}$$

Equation (3.2) is the Reynolds equation in non-dimensional form.

Considering $\bar{h}$ as the function of θ only and differentiating with respect to θ

$$\bar{h}^3\frac{\partial^2\bar{p}}{\partial\theta^2}+3\bar{h}^2\frac{\partial\bar{p}}{\partial\theta}\frac{\partial\bar{h}}{\partial\theta}+\left(\frac{D}{L}\right)^2\bar{h}^3\frac{\partial^2\bar{p}}{\partial\bar{z}^2}=\frac{d\bar{h}}{d\theta} \tag{3}$$

Now Eqn. (3.3) has been discretized using central difference quotients to arrives at

$$\bar{p}_{i,j}=\frac{\left[\left(\bar{p}_{i+1,j}-\bar{p}_{i-1,j}\right)+\left(\frac{D}{L}\right)^2\left(\frac{\Delta\theta}{\Delta\bar{z}}\right)^2\left(\bar{p}_{i,j+1}+\bar{p}_{i,j-1}\right)-\frac{3\varepsilon}{2\bar{h}}\left(\bar{p}_{i+1,j}-\bar{p}_{i-1,j}\right)(\Delta\theta)\sin\theta+\frac{\varepsilon\sin\theta}{\bar{h}^3}(\Delta\theta)^2\right]}{2\left[1+\left(\frac{D}{L}\right)^2\left(\frac{\Delta\theta}{\Delta\bar{z}}\right)^2\right]} \quad (4) \quad 2.4$$

Boundary conditions:

1. $\bar{p}_i(\theta,\bar{z})=0$ at $\theta=0^0$ and $\theta=360^0$

2. Pressure at the end of bearing are assumed to be zero (atmospheric) $\bar{p}_i(\theta,\pm1)=0$

3. The pressure distribution is symmetrical about the mid plane of bearing.

4. $\frac{\partial\bar{p}_i}{\partial\theta}=0$ at $\theta=\theta_2$ and $\bar{p}=0$ at $\theta=\theta_2$.

Where, $\theta_2>\pi$

θ_2 is the angle at which film ruptures/cavitates.

Since the bearings considered here for analysis are symmetrical about their central plane ($\bar{z}=0$), only one half of the bearings needs to be considered.

Non dimensional load carrying capacity:

Non-dimensional steady state load component are given by

$$\bar{W}_X=\int_0^1\int_0^{2\pi}\bar{p}\cos\theta d\theta d\bar{z}$$

$$\bar{W}_Y=\int_0^1\int_0^{2\pi}\bar{p}\sin\theta d\theta d\bar{z}$$

Resultant load carrying capacity is given as

$$\bar{W}=\sqrt{\bar{W}_X^2+\bar{W}_Y^2} \quad (5)$$

Sommerfeld number:

$$S=\frac{\eta N}{P}\left(\frac{R}{c}\right)^2 \quad (6)$$

Since $dz=\frac{L}{2}\bar{z}d\bar{z}$;

when $z=-\frac{L}{2}$, then $\bar{z}=-1$ and when $z=\frac{L}{2}$, then $\bar{z}=1$

Using substitution equation (2.10) arrives at

$$\bar{S}=\frac{1}{6\pi\bar{W}} \quad (7)$$

Non-dimensional flow:

Assuming $u_a + u_b$ is almost equal to u and integrating from $-\frac{L}{2}$ to $+\frac{L}{2}$ we will arrives at

$$q_{in} = \bar{q}_{in} \pi NDLC \quad (8)$$

Optimization Technique (Artificial Bee Colony):

Artificial Bee Colony (ABC) is a relatively new member of swarm intelligence. It is one of the most recently defined algorithms, motivated by the intelligent behavior of honey bees. It is as simple as Particle Swarm Optimization (PSO) and Differential Evolution (DE) algorithms, and uses only common control parameters such as colony size and maximum cycle number. ABC as an optimization tool provides a population-based search procedure in which individuals called foods positions are modified by the artificial bees with time and the bee's aim is to discover the places of food sources with high nectar amount and finally the one with the highest nectar.

3.3 Agents in ABC:

- The Employed Bee:
  The Employed Bee stays on a food source and provides the neighbourhood of the source in its memory.
- The Onlooker Bee:
  The Onlooker Bee gets the information of food sources from the employed bees in the hive and select one of the food source to gathers the nectar.
- The Scout:
  The Scout is responsible for finding new food, the new nectar and sources.

3.4 Flowchart of the Artificial Bee Colony algorithm:

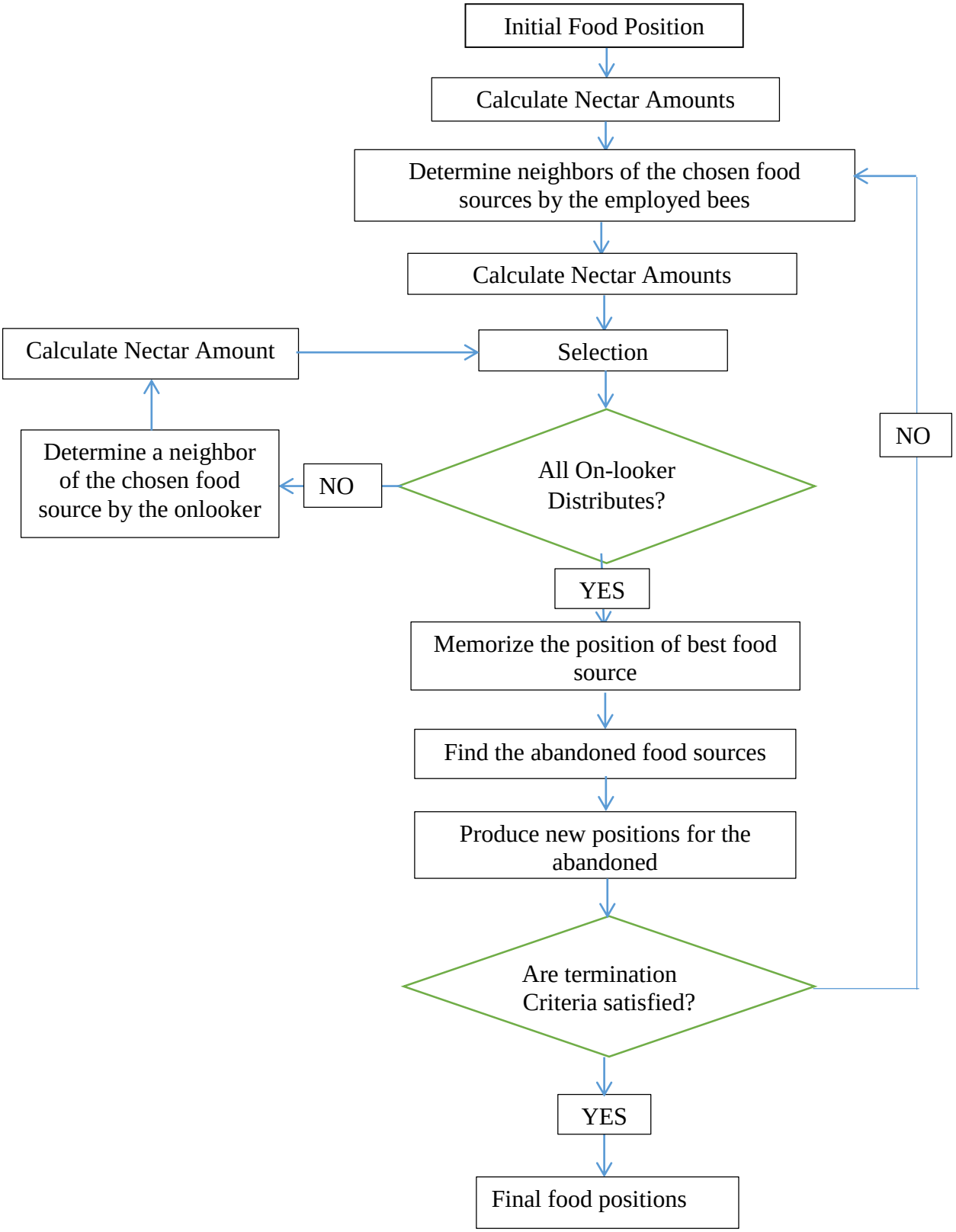

RESULTS AND DISCUSSION

In table (1) comparison of maximum load carrying capacity for various L//D ratio with varying eccentricity ratio is shown. For a particular L/D ratio, as the eccentricity ratio increases the maximum load carrying capacity also increases and for a particular eccentricity ratio as the L/D ratio decreases, maximum load carrying capacity also decreases.

Table 1: Maximum Load Carrying Capacity for Various L/D Ratio.

Eccentricity Ratio (ε)	$\bar{W}$ for L/D=1	$\bar{W}$ for L/D=0.5	$\bar{W}$ for L/D=0.25
0.1	0.0402	0.0122	0.0032
0.3	0.1356	0.0430	0.0117
0.5	0.2941	0.1033	0.0294
0.7	0.6746	0.2849	0.0896
0.9	2.7966	1.6939	0.7159

In table (2) comparison of minimum friction variable for various L//D ratio with varying eccentricity ratio is shown. For a particular L/D ratio, as the eccentricity ratio increases the minimum friction variable decreases and for a particular eccentricity ratio as the L/D ratio decreases, maximum load carrying capacity increases.

Table 2: Minimum Friction Variable for Various L/D Ratio.

Eccentricity Ratio (ε)	$\overline{F}$ for L/D=1	$\overline{F}$ for L/D=0.5	$\overline{F}$ for L/D=0.25
0.1	28.0121	92.7112	348.45
0.3	8.6335	27.2974	100.72
0.5	4.3633	12.5134	44.05
0.7	2.2710	5.4680	17.47
0.9	1.0848	1.4466	3.5218

In table (3) comparison of maximum flow co-efficient for various L//D ratio with varying eccentricity ratio is shown. For a particular L/D ratio, as the eccentricity ratio increases the maximum load carrying capacity also increases and for a particular eccentricity ratio as the L/D ratio decreases, maximum load carrying capacity increases.

Table 3: Maximum Non-Dimension Flow Co-efficient for Various L/D Ratio.

Eccentricity Ratio (ε)	$\overline{Q}$ for L/D=1	$\overline{Q}$ for L/D=0.5	$\overline{Q}$ for L/D=0.25
0.1	0.1601	0.1785	0.1844
0.3	0.4512	0.5008	0.5161
0.5	0.7062	0.7760	0.7969
0.7	0.9106	0.9954	1.0176
0.9	1.0753	1.0539	1.1173

In fig. 1,2 and 3 variation of Maximum Load Carrying Capacity, Minimum Friction Variable and Maximum Flow Co-efficient has been shown respectively for L/D=1. The location of groove for corresponding θ_1 and θ_2 is also mentioned.

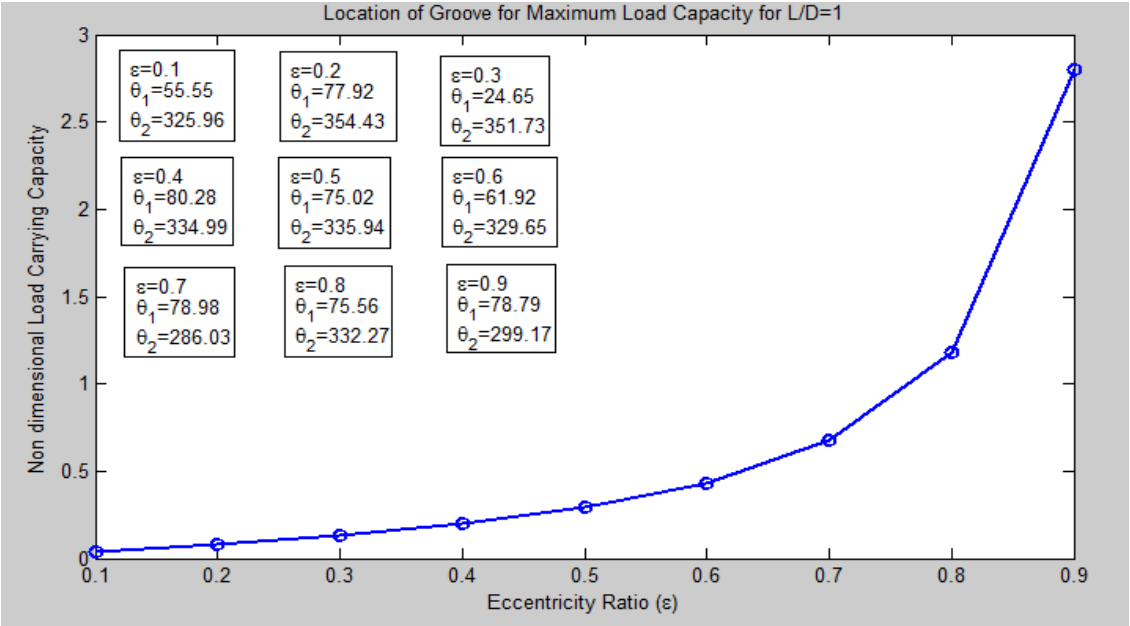

Fig 1: Variation of Maximum Load Carrying Capacity with Eccentricity Ratio for L/D=1.

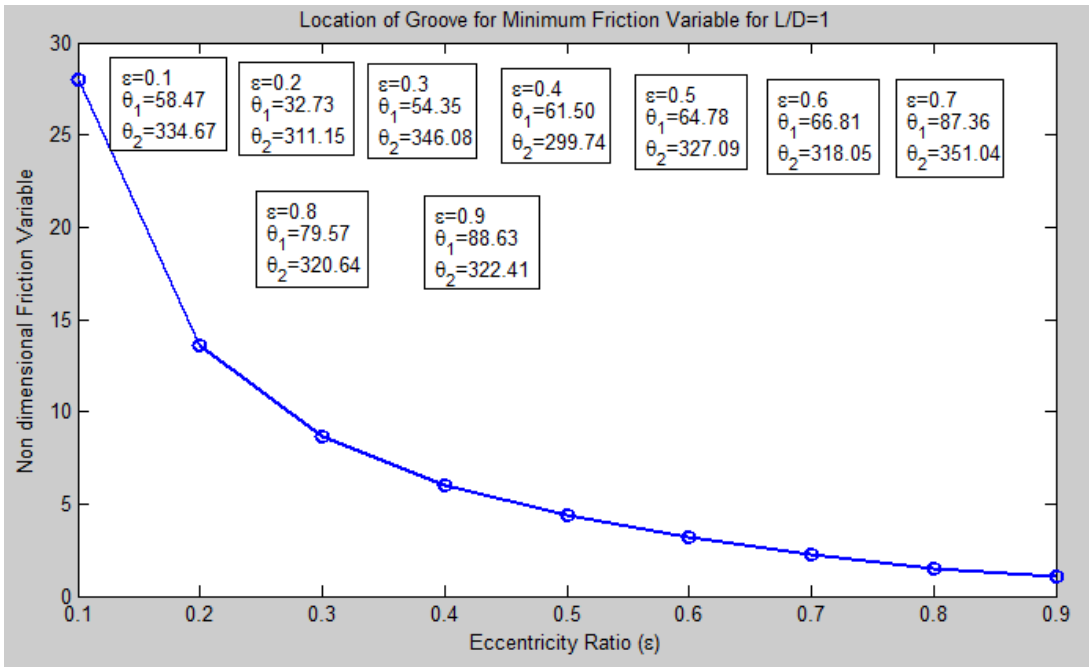

Fig 2: Variation of Minimum Friction Variable with Eccentricity Ratio for L/D=1.

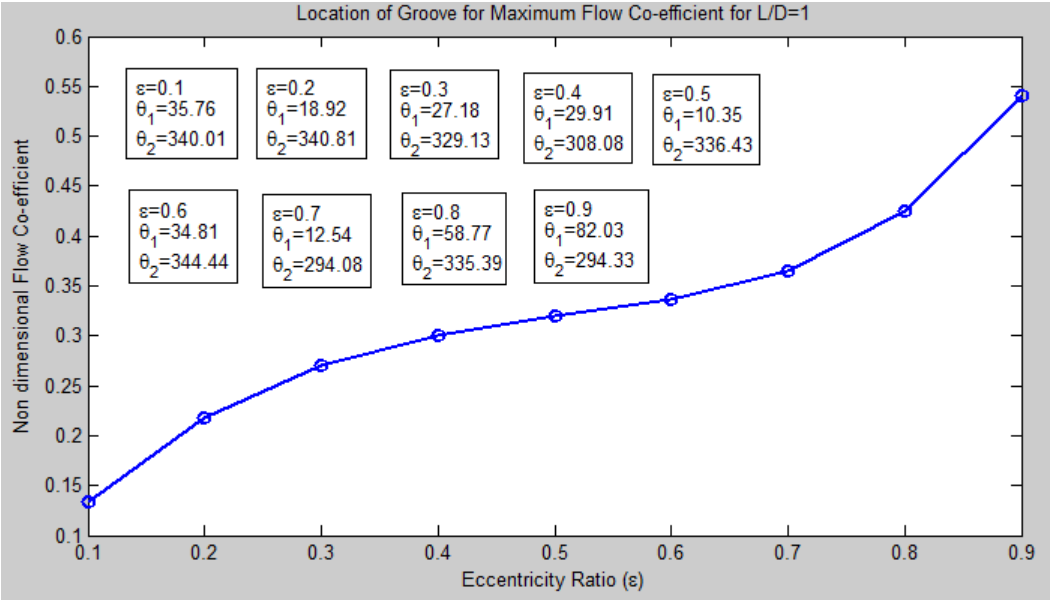

Fig 3: Variation of Maximum Flow Co-efficient with Eccentricity Ratio for L/D=1.

In fig. 4,5 and 6 variation of Maximum Load Carrying Capacity, Minimum Friction Variable and Maximum Flow Co-efficient has been shown respectively for L/D=0.5. The location of groove for corresponding θ_1 and θ_2 is also mentioned.

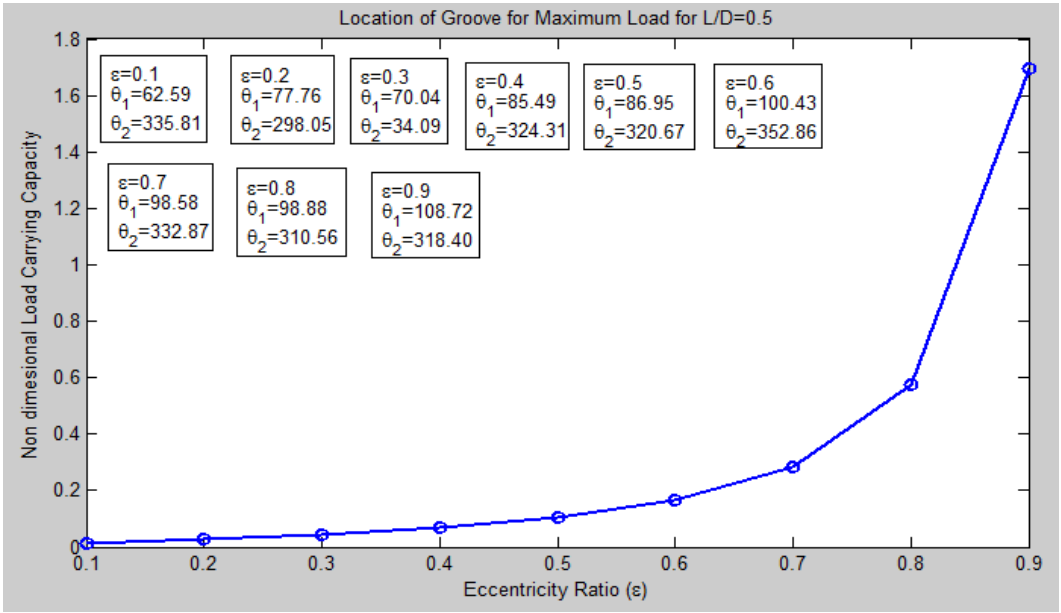

Fig 4: Variation of Maximum Load Carrying Capacity with Eccentricity Ratio for L/D=0.5

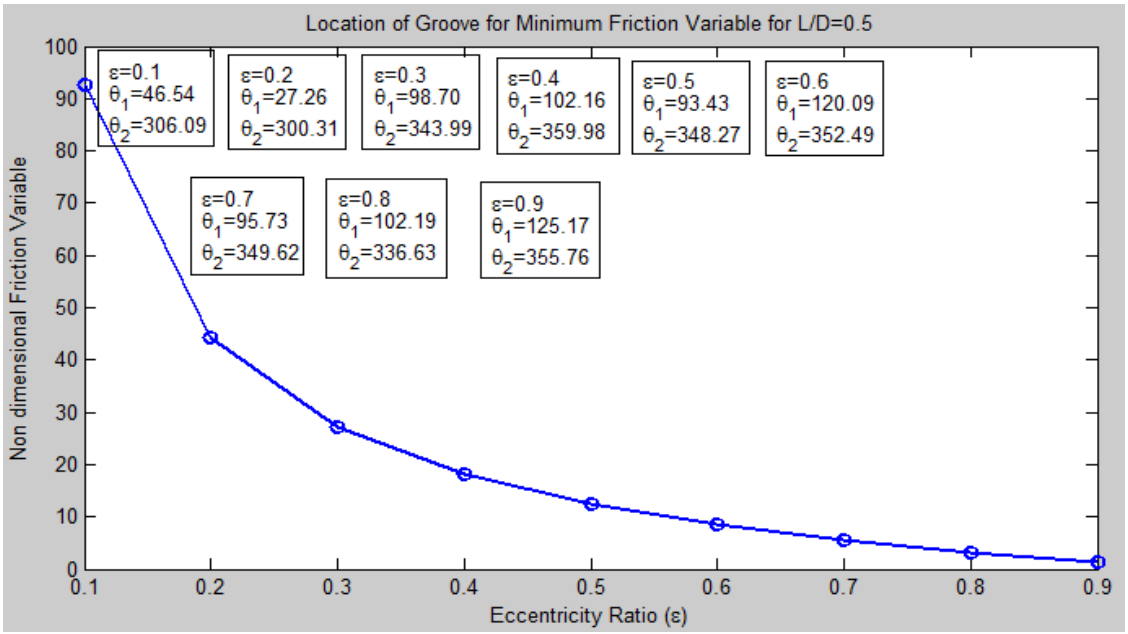

Fig 5: Variation of Minimum Friction Variable with Eccentricity Ratio for L/D=0.5.

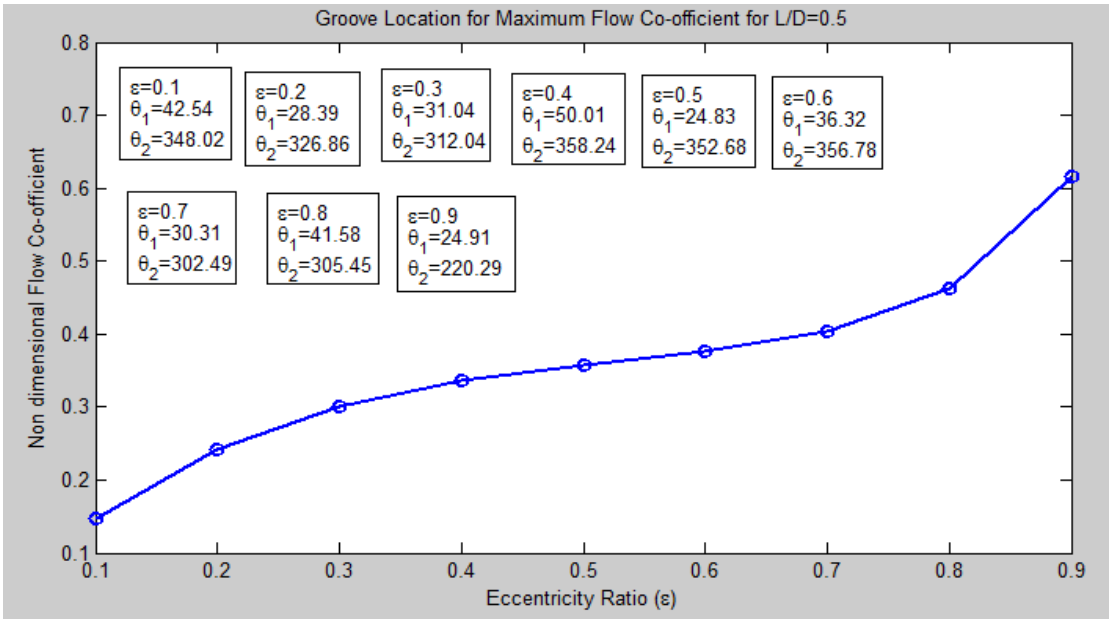

Fig 6: Variation of Maximum Flow Co-efficient with Eccentricity Ratio for L/D=0.5.

In fig. 7,8 and 9 variation of Maximum Load Carrying Capacity, Minimum Friction Variable and Maximum Flow Co-efficient has been shown respectively for L/D=0.25. The location of groove for corresponding θ_1 and θ_2 is also mentioned.

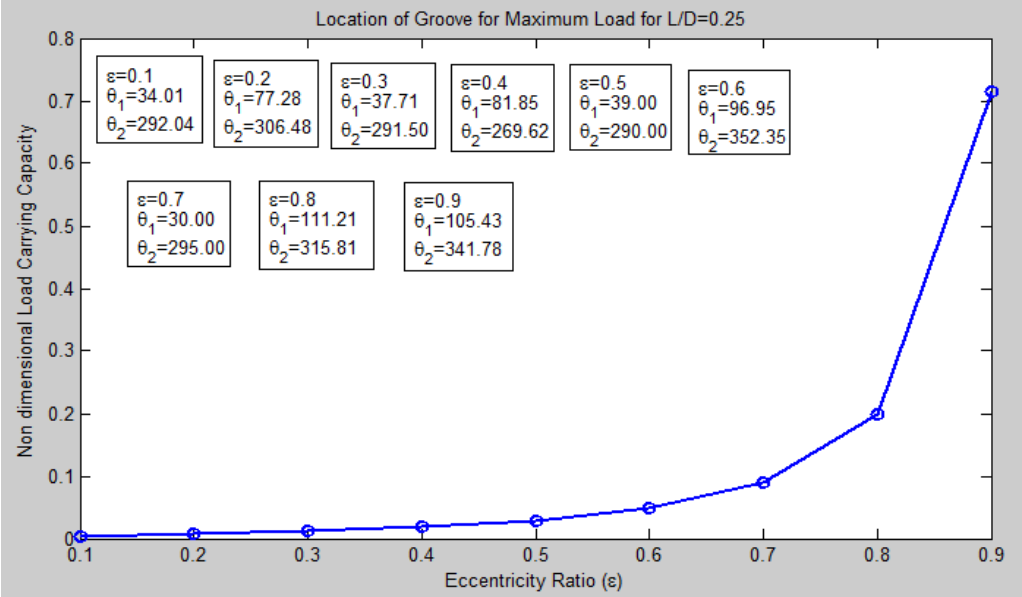

Fig 7: Variation of Maximum Load Carrying Capacity with Eccentricity Ratio for L/D=0.25.

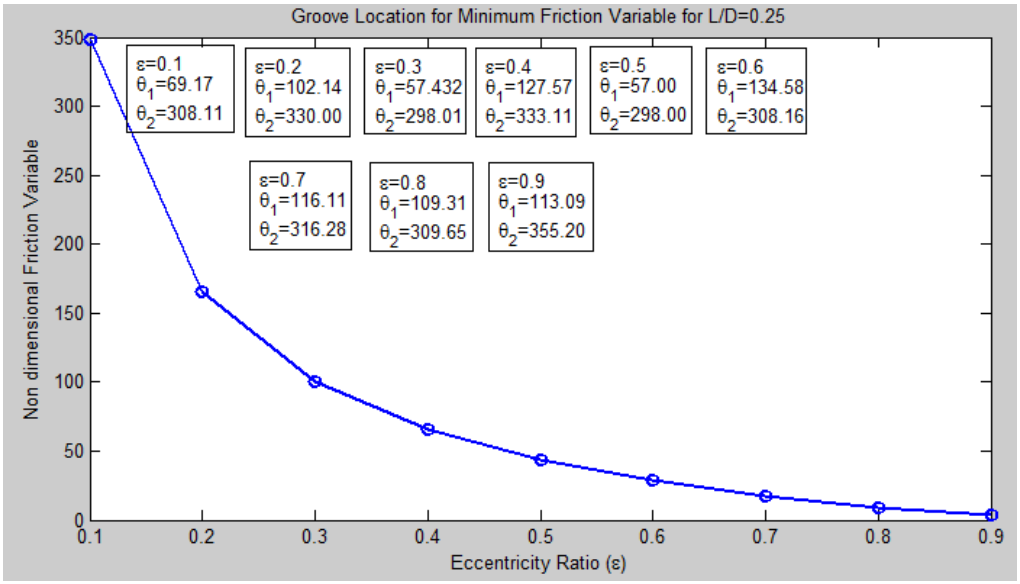

Fig 8: Variation of Minimum Friction Variable with Eccentricity Ratio for L/D=0.25.

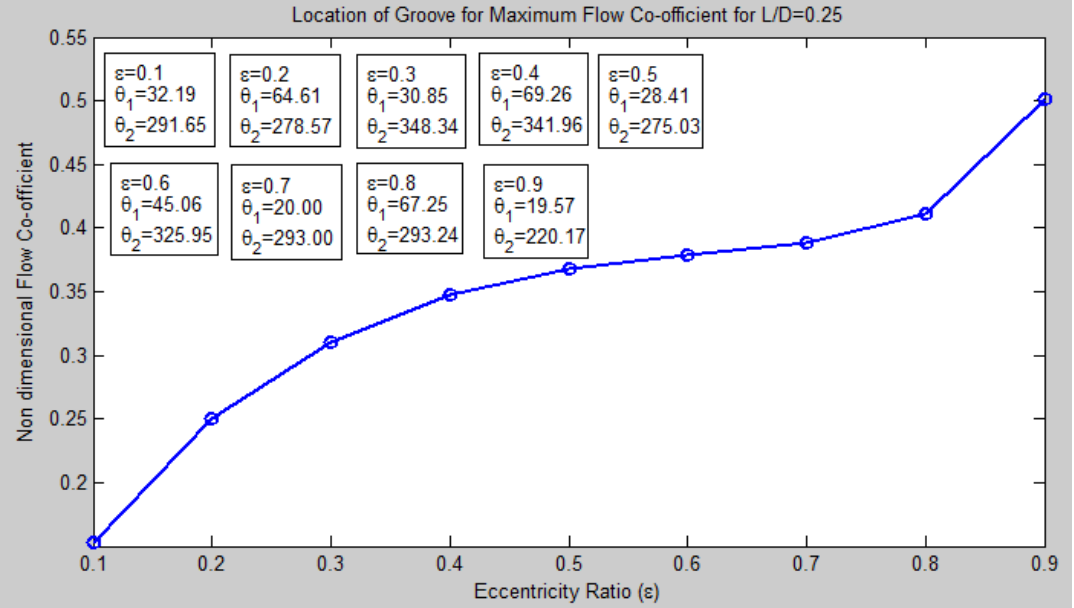

Fig 9: Variation of Maximum Flow Co-efficient with Eccentricity Ratio for L/D=0.25.

CONCLUSION:

From the results presented here, it can be inferred that the both first and second groove location are sensitive to the type of objective function. It can be seen from the result that the location of the groove at diametrically opposite position (180^0 apart from each other) does not lead to the optimum value for the any of the objective function. Experimental verification would result to the production of bearings with optimum groove locations, however, it is beyond the scope of the present work. The present study would give a scope for researcher for the experimental validation which would lead to the bearing with optimum performance.

Nomenclature:

c = Radial clearance (m)
D = Journal diameter (m)
L = Length of bearing (m)
p = Unit loading (KN/m^2)
Q = Volume flow rate (m^3/s)
R = Bearing radius (m)
S = Sommerfeld number
U = Linear velocity (m/s)
W = Load carrying capacity (KN)
$\bar{W}$ = Non-dimensional load carrying capacity
W_x = Horizontal component of the resultant load (KN)
W_y = Vertical component of the resultant load (KN)
$\bar{W}_X$ = Non-dimensional vertical component of resultant load (KN)
$\bar{W}_X$ = Non-dimensional horizontal component of resultant load (KN)
f = Coefficient of friction
t = Time (s)
h = Film thickness (m)
$\bar{h}$ = Non-dimensional film thickness
p = Pressure (Pa)
$\bar{p}$ = Non-dimensional pressure
q = Volume flow rate per unit length
$\bar{q}$ = Non-dimensional flow coefficient
θ = Angular coordinate
θ_1 = Location of First Groove
θ_2 = Location of Second Groove
ϕ = Attitude angle (radian)
ω = Angular velocity (rad/s)
η = Absolute viscosity (Pa-s)
N = Revolution per unit time
x, y, z = Cartesian co-ordinates
Δ = Mesh size

REFERENCE:

[1] A. A. Raimondi and John Boyd, 1958, "*A solution for the finite journal bearing and its application to analysis and design.*" ASLE Transactions, Vol. 1, PP 159-174 and Available online: 2011.

[2] D. Vijayraghavan and T. G. Keith, 1992, "*Effect of type and location of oil groove on the performance of journal bearings.*" STLE Tribology Transactions, Vol. 35, PP 98-106.

[3] G.H. Jang and J.W. Yoon, 2002, "*Nonlinear dynamic analysis of a hydrodynamic journal bearing considering the effect of rotating or stationary herringbone groove*", Transaction of the ASME, Journal of Tribology, Vol. 124, PP 297-304.

[4] H. Hirani and T. V. V. L. N. Rao, 2003, "*Optimization of Journal Bearing Groove Geometry Using Genetic Algorithm.*" National Conference on Machines and Mechanism (NaCoMM).

[5] Pei-Wei Tsai, Jeng-Shyang Pan, Bin-Yih Liao and Shu-chuan chu, 2009, "*Enhanced Artificial Bee Colony Optimization*", International journal of innovative computing, information and control, Vol. 5, PP 1349-4198.

[6] R. Murugan and M.R. Mohan, 2012, "*Artificial bee colony optimization for the combined heat and power economic dispatch problem*", ARPN journal of engineering and applied science, Vol. 7, ISSN 1819-6608.

[7] A. Bahriye and K. Dervis, 2012, "*A modified artificial bee colony algorithm for real parameter optimization*", Information Science, Vol. 192, PP 120-142.

[8] K. Dervis and A. Bahriya, 2009, "*A comparative study of artificial bee colony algorithm*", Applied Mathematics and computation, Vol. 214, PP 108-132.

[9] Cho, M.R., and Shin, H.J., and Han, D.C., 2007 "*A Study on the Circumferential Groove Effects on the Minimum Oil Film Thickness in Engine Bearings.*" KSME International Journal, Vol. 14, PP 737-743.

[10] Sherbiny, M.E. and F. Salem, and Hafinaway, N.E., June 1984, "*Optimum design of hydrostatic journal bearings part I: maximum load capacity"*, J. International, Vol. 17, Issue 3, Pages 155-161.